Off-Axis Co-Optical Path Large-Range Line Scanning Chromatic Confocal Sensor

Meizhong LIAO[1,2], Yuqi YANG[1,2], Xiaolian LU[1,2], Haiqi LI[1,2], Jun ZHANG[1,2*], Jinfeng WANG[3], and Zhe CHEN[1,2]

[1]*Guangdong Provincial Engineering Technology Research Center on Visible Light Communication, Jinan University, Guangzhou 510632, China*

[2]*Guangzhou Municipal Key Laboratory of Engineering Technology on Visible Light Communication, Jinan University, Guangzhou 510632, China*

[3]*Dongguan Shenzhou Vision Technology Co., Ltd., Dongguan 523127, China*

[*]Corresponding author: Jun ZHANG E-mail: tzhangjun_oe@jnu.edu.cn

Abstract: This article proposes a line scanning chromatic confocal sensor to solve the problem of limited chromatic confocal measurement due to the small measurement range and low measurement efficiency in the industrial inspection process. To obtain an extensive dispersion range, the advantages of a simple single-axis structure are combined with the advantages of a large luminous flux of a biaxial structure. Considering large-scale measurement, our sensor uses off-axis rays to limit the illumination path and imaging path to the same optical path structure. At the same time, the field of view is expanded, and a symmetrical structure is adopted to provide a compact optical path and improve space utilization. The simulation and physical system test results shows that the sensor scanning line length is 12.5 mm, and the axial measurement range in the 450 nm to 750 nm band is better than 20 mm. The axial resolution of the detector is ±1 μm combined with the subpixel centroid extraction data processing method, and the maximum allowable tilt angle for specular reflection samples is ±7°. The thicknesses of transparent standard flat glass and the wet collagen membrane are measured. The maximum average error is 1.3 μm, and the relative error is within 0.7%. The constructed sensor is of great significance for rapidly measuring the three-dimensional profile, flatness, and thickness in the fields of transparent biological samples, optics, micromechanics, and semiconductors.

Keywords: Chromatic confocal sensor; optical design; off-axis co-optical path; line scanning

Citation: Meizhong LIAO, Yuqi YANG, Xiaolian LU, Haiqi LI, Jun ZHANG, Jinfeng WANG, *et al*., "Off-Axis Co-Optical Path Large-Range Line Scanning Chromatic Confocal Sensor," *Photonic Sensors*, 2024, 14(3): 240309.

1. Introduction

Many fields require measuring the surface topography and thickness of products, such as the industrial manufacturing of glass, rolled metal, optical components, semiconductors, or micromachined integrated circuits, and all fields require products with a flat surface and a uniform thickness. Standard measurement technologies can be divided into two categories: contact measurement and noncontact measurement. Contact measurement can easily cause damage to the workpiece's surface

Received: 17 October 2023 / Revised: 4 January 2024

DOI: 10.1007/s13320-024-0713-5
Article type: Regular

during the measurement process and is extremely sensitive to external interference [1, 2]. Due to these shortcomings, it is unsuitable for continuous and rapid inspection of production lines. In contrast, the noncontact detection technology with nondestructive measurement characteristics shows unique advantages. The chromatic confocal measurement technology [3–5] has been widely used in defect detection, surface testing, and thickness detection due to its excellent resolution characteristics and stray light suppression capabilities. This technique has been widely used for applications such as roughness measurement, three-dimensional topography reconstruction [6], displacement measurement, and thickness measurement [7]. The chromatic confocal measurement technology is derived from laser confocal microscopy and overcomes the problem of low measurement efficiency caused by the laser confocal microscope scanning layer by layer in the axial direction [8]. This chromatic confocal measurement technology fully uses the chromatic expansion characteristics of the dispersive objective lens, it reflects the topography of the measured surface based on the measured surface's reflection (or transmission) wavelength information.

Line scanning systems can achieve faster sampling speed than point-scanning chromatic confocal systems that require a two-dimensional displacement stage. The line scanning chromatic confocal microscopy system utilizes the slit scanning confocal microscopy technology, and two types of systems have been developed: the single-axis [9–16] and biaxial [17–22]. With the development of the semiconductor technology and materials science, the emergence of high-speed detectors, supercontinuum light sources, and other devices has made it possible to further improve the performance of chromatic confocal measurement systems [23, 24]. To pursue the measurement goals of an extensive dispersion range and high dispersion linearity, scholars have conducted much research on the dispersion objective lens in the core of the system and proposed many new design strategies and possibilities. In 2017, Cui *et al*. [25] designed a dispersive objective lens using the concept of separating dispersion and focusing functions. By matching different focusing objectives, the measurement ranges of 1 300 μm and 225 μm were obtained, and the corresponding axial resolution was 2 μm and 0.4 μm, respectively. In 2021, Yang *et al*. [26] proposed a design model for quantitative anti-dispersion objective lenses, which concealed the multiple structures that controlled axial linear dispersion in a single structure and unified the reference plane for image quality evaluation; additionally, the dispersion linear determination coefficient of the dispersion objective lens was 0.999 8. In 2021, Zhang *et al*. [27] proposed a theory of classifying doublet lenses according to optical power distribution and divided the doublet lenses into the L-type and S-type. They concluded that S-type doublet lenses were suitable for designing objective lenses of larger numerical apertures, and the L-type was more suitable for designing objective lenses with a broader dispersion range. In 2022, Liu *et al*. [28] designed a chromatic confocal measurement system based on the Fresnel zone plate (FZP). The axial measurement range of the system exceeded 16 mm, the axial resolution reached 0.8 μm, and the displacement measurement accuracy was excellent at 0.4%. In recent years, the spectral confocal measurement technology studies have been flourishing. Although the point-based spectral confocal measurement system has high resolution, its measurement range is limited, and the measurement time is long, so it cannot meet the requirements of the online detection of large area objects. Although line-scan spectral confocal measurement has improved scanning speed, it still cannot meet the multiple requirements of the high linearity, large measurement range, high integration, low cost, and stability.

Combining the advantages of uniaxial and

biaxial structures, in this study, an off-axis large-range line scanning color confocal sensor (LSCCS) is designed. For the phenomenon of low light energy utilization caused by the small luminous flux in the existing linear scanning single-axis optical path structure, the difficulties of triangular optical path structure installation, and high equipment construction cost in the biaxial optical path structure, the symmetrical dispersion objective, which is separated from the illumination path and the imaging path, is designed without using the beam splitter while maintaining the uniaxial common optical path structure. The off-axis beam solves the problem of energy loss, reduces the signal crosstalk, and compact the system structure.

2. Line scanning chromatic confocal sensor measurement principle and performance indicators

The measurement principle of the chromatic confocal sensor is to introduce the spectral dimension-color-coding technology based on laser confocal microscopy. The sensor uses light of different wavelengths to produce axial dispersion of sufficient distance after passing through the objective lens. Then, it analyzes the spectrum of the emitted light to achieve an axial depth measurement of the sample. Furthermore, to solve the problem of low single-point measurement efficiency, slits are used to replace pinholes, and area array sensors are used to replace line array sensors. This is the LSCCS.

2.1 Optical path structure

The line scanning chromatic confocal measurement system is shown in the left picture of Fig. 1. The light emitted by the broad spectrum light source passes through the optical fiber bundle and the cylindrical lens to form a line light source, which is incident on the slit. The light emitted from the slit enters the dispersive objective lens. The dispersion objective lens's specially designed axial chromatic aberration is used to obtain the dispersion distribution along the optical axis. Different depths on the sample surface reflect light of different wavelengths, and the morphology of the sample surface is reversed through the spectral analysis of the reflected light.

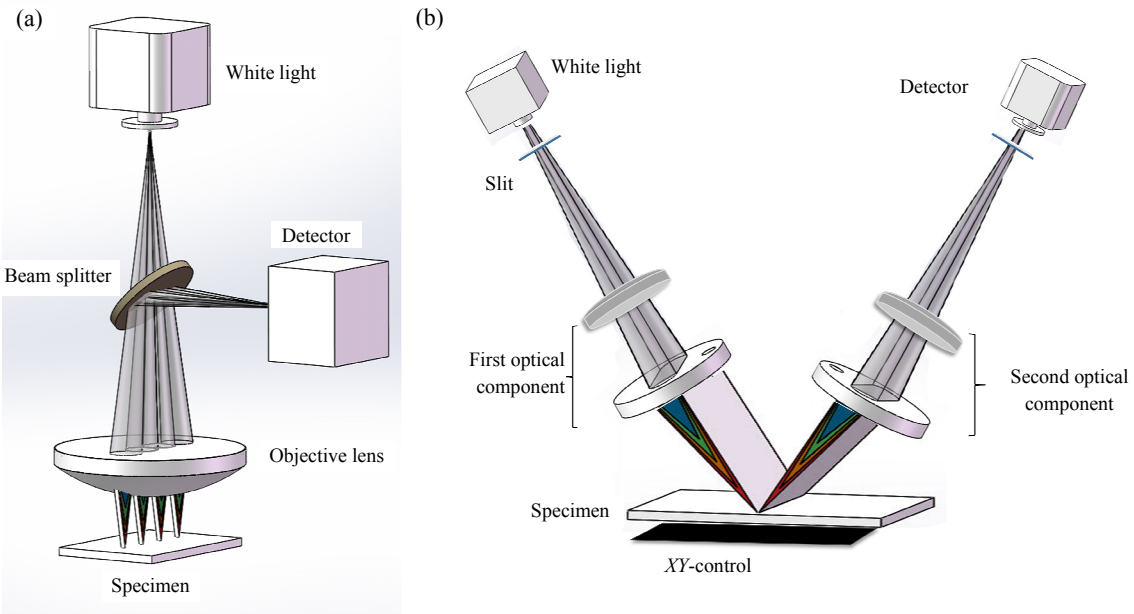

Fig. 1 Line scanning chromatic confocal sensor with different optical path structures: (a) single-axis optical path structure based on the splitter prism type and (b) triangular two-axis optical path structure.

Line scanning chromatic confocal measurement systems adopt the two structures shown in Fig. 1. The single-axis structure in the left picture of Fig. 1(a) is based on the laser confocal system, which directly replaces the pinhole with a slit. In contrast to the laser confocal system, the incident light and outgoing light have different wavelengths. In the line scanning chromatic confocal measurement system, the reflected light has the same wavelength range as the incident light. If the incident light and the outgoing light use the same optical path, the light energy entering the detector will be significantly reduced due to the spectroscope; the crosstalk between the optical paths will be severe, thus reducing the measurement accuracy. Therefore, the biaxial chromatic confocal sensor has a dual optical path structure in which the incident light and outgoing light are separated (as shown on the right side of Fig. 1(b). However, this inevitably introduces two sets of optical path structures, which increases the system volume and cost, and causes difficulties in its assembly and adjustment. In this study, the simplicity of the single-axis structure is combined with the high throughput of the dual-axis structure. An off-axis single optical path structure is proposed, as shown in Fig. 2. The off-axis beam separates the incident and outgoing light in the single-axis optical system, ensuring significant luminous flux detection while achieving confocal measurement.

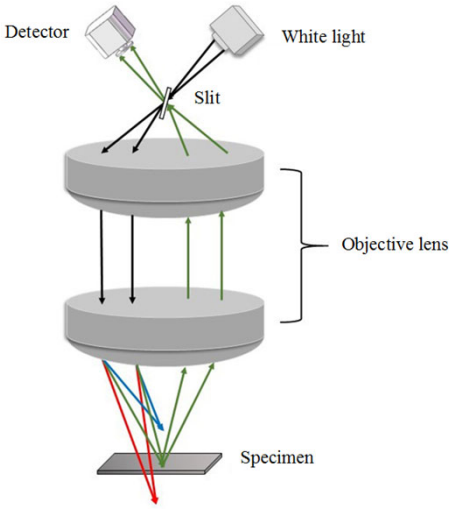

Fig. 2 Off-axis single optical path structure.

2.2 Performance indicators

The primary purpose of the LSCCS is to measure the surface shape and thickness of the sample. Therefore, the first important performance indicator is the measurement range. L_Z is the measurement range in the depth direction of the LSCCS; it is the core parameter of the system design. Its size is determined by the working band of the light source and the dispersion capability of the confocal optical system. The light from the wide-spectrum light source passes through the dispersion objective lens and is dispersed in the direction of the optical axis. The measurement range is the physical distance between the minimum wavelength and the maximum wavelength ($\lambda_{\min}$ to $\lambda_{\max}$) on the optical axis [Fig. 3(a)]. L_Z is expressed as follows:

$$L_Z = l'(\lambda_{\max}) - l'(\lambda_{\min}) \tag{1}$$

where $l'(\lambda)$ is the image distance. Different from the general lens design, the dispersion objective lens group of the LSCCS needs to retain the axial chromatic aberration and provide a linear relationship of the axial chromatic aberration with respect to the wavelength. Specifically, this is defined as (2):

$$\mathrm{d}l' = l'(\lambda + \mathrm{d}\lambda) - l'(\lambda) = K\mathrm{d}\lambda \tag{2}$$

where K is a constant and equivalent to the linear dispersion coefficient. Since the relationship between the refractive index of glass and wavelength is nonlinear for a lens made of a single material, the dispersive objective lens must adopt a design structure that combines lenses of multiple materials to meet the linear requirement between the axial chromatic aberration and wavelength. When the dispersive objective lens is composed of N lenses, using the axial dispersion between F light (λ=486.1 nm), D light (λ=587.6 nm), and C light (λ=656.3 nm) as an example, record $\mathrm{d}l'_{\mathrm{FC}} = l'_{\mathrm{F}} - l'_{\mathrm{C}}$ and $\mathrm{d}l_{\mathrm{FC}} = l_{\mathrm{F}} - l_{\mathrm{C}}$:

$$\mathrm{d}l'_{\mathrm{FC}} = \beta^2 \mathrm{d}l_{\mathrm{FC}} - (1-\beta)^2 \varphi^{-2} \sum_{i=1}^{N} \left(\varphi_{\mathrm{D}_i} / \upsilon_{\mathrm{D}_i} \right) \tag{3}$$

where $\beta = l'/l$ represents the lateral magnification

of the optical system; l and l' are the object distance and image distance, respectively; φ is the power of the dispersive objective lens; $\varphi_{D_i} = \left(n_{D_i} - 1\right)\Delta C_i$ is the power of the D light of the ith lens, where $n_{(\cdot)_i}$ is the refractive index of the $(\cdot)$ light of the ith single lens and ΔC_i is the curvature difference between the front and rear surfaces of the ith single lens; $\upsilon_{D_i} = (n_{D_i} - 1)/(n_{F_i} - n_{C_i})$ is the Abbe number of the ith lens. The theoretical result of the axial chromatic aberration can be analyzed according to the above formulas [29].

From the analysis of the above equation, the more types of glass materials that make up the dispersive lens group, the easier it is to achieve the high linearity chromatic aberration. However, the excessive axial chromatic aberration will also lead to an increase in the length of the system. Therefore, the design of the dispersive objective lens group needs to use appropriate glass materials and reasonable optical power.

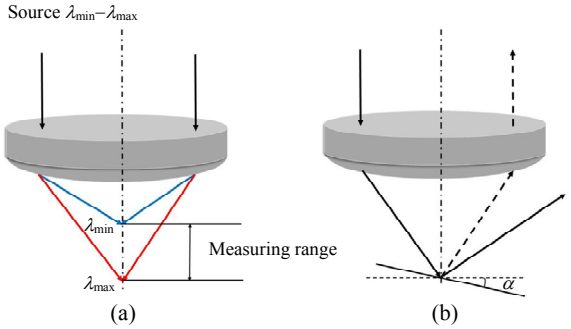

Fig. 3 Parameter diagram of line scanning spectral color confocal sensor: (a) measuring range and (b) maximum tilt angle.

The second key indicator, linearity, refers to the degree of linear correlation between the wavelength and displacement within the measurement range. High linearity ensures consistent measurement accuracy at each wavelength. The system's linearity is typically assessed using the regression analysis, with the least squares method to linearly fit the wavelength and displacement. The correlation coefficient R^2 is used for evaluation. When the correlation coefficient R^2 is closer to 1, the better linearity and more accessible subsequent signal analysis and image processing are obtained.

The third performance indicator is the maximum tilt angle. The criterion for determining the depth information of the sample surface by the chromatic confocal system is the wavelength information of the light reflected back from the sample. If the detection end cannot receive the light reflected back from the sample, it cannot be measured. As shown in Fig. 3(b), when the sample surface is not tilted, the light incident at a normal angle can be reflected back to the dispersive objective lens. However, the sample surface has a tilt angle of α, the light cannot be reflected back to the dispersive objective lens, and the detection end will not be able to obtain the signal, so the surface information of the sample cannot be obtained. To get accurate and practical results of the sample to be tested, sufficient light energy should be ensured to enter the detection end. As the tilt angle of the sample increases, the light energy that the dispersive objective lens can receive decreases. Therefore, the angle, at which the sample is to be measured cannot reflect the incident light into the dispersive objective lens, is defined as the maximum tilt angle.

3. Design and analysis of dispersive objective lenses

The axial dispersion capability of the LSCCS not only determines the dispersion range and measurement capabilities but also restricts the measurement accuracy and sensitivity of the system. Since general biological materials are highly transparent and low-refractive materials, if the imaging axis is perpendicular to the object's surface to be measured, the reflected light will be feeble, resulting in a low signal-to-noise ratio and affecting the measurement performance of the system. Therefore, an off-axis optical path design is used to separate the imaging path from the illumination path. Since a slit is used in the optical path to realize line scanning, to take into account the entire line field of view and ensure that all the light emitted from the slit can enter the dispersive objective lens, the

effective aperture of the dispersive objective lens is more considerable. A large-diameter lens also means that the radius of the lens is large, so the radius of curvature cannot be too small. Otherwise, the focusing and divergence capabilities of the lens will be reduced. In addition, large dispersion objective lenses will introduce more significant aberrations. According to the axial dispersion formula given by (3) and the previous analysis, this article uses a spherical lens combination of easy-to-process high dispersion refractive materials to design the dispersion objective lens. The objective lens is designed by adding the multi-lens combination design to meet the performance requirements of the LSCCS. At the same time, to make the optical path structure compact, improve space utilization, and avoid a large and complex system, the field of view is expanded while taking into account a considerable measurement range, and a symmetrical structure is adopted to limit the illumination path and imaging path to the same optical path structure, which not only solves the problem of receiving reflected light but also makes full use of the large aperture lens group.

The simulation design is carried out in ZEMAX optical design software, and the final designed structure of the dispersion objective lens group is shown in Fig. 4. Specifically, the entire dispersive lens group consists of 14 lenses; here, 1–7 lenses form the first-stage dispersive objective lens group, and 8–14 lenses form the second-stage dispersive objective lens group. When optimizing the design of the objective lens to limit the angle of incident light in the dispersive objective lens, reduce the assembly difficulty of the actual system, and effectively filter out the interference light in the non-detection surface, thereby improving the imaging quality, the apertures are added to the lens group. The apertures A1, A2, and A3 are respectively located in front of the first-stage dispersion objective lens group, between the two sets of dispersion objective lens groups and behind the second-stage dispersion objective lens group. The two-stage dispersion objective lens groups are coaxially arranged. The aperture has two channels for light input and output, and the three apertures are circular light-shielding diaphragms that are symmetrical about the optical axis. The linear light emitted from the slit at an inclination angle of 15° passes through aperture A1, enters the light entrance of aperture A2 from one side of the first-stage dispersion objective lens group, and then passes through one side of the second-stage dispersion objective lens group. After that, it reaches the entrance channel of aperture A3 and finally reaches the surface of the object under test. The light reflected by the object's surface to be measured will exit through the symmetrical side opposite to the dispersion objective lens group as mentioned above and the light outlet of the diaphragm of A1, and finally be transmitted to the spectroscopic system through the slit again.

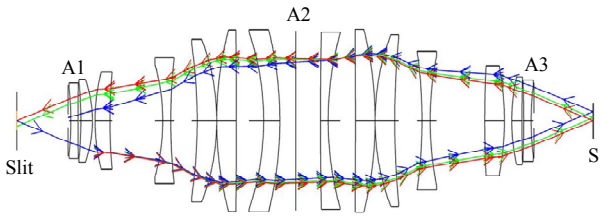

Fig. 4 Structure and optical path diagram of dispersion objective lens.

The axial chromatic aberration of the large-range dispersion objective lens group is 20 mm. The spot diagram is an essential standard for measuring the performance indicators of optical systems. Figure 5 shows the spot diagram at the focus positions of 450 nm, 600 nm, and 750 nm in the central and edge fields of view. The black circle represents the Airy disk.

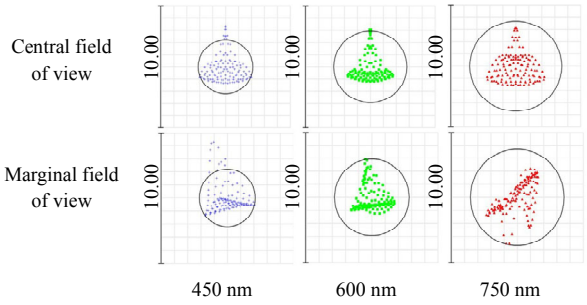

Fig. 5 Spot diagrams at different wavelengths.

At the wavelengths of 450 nm, 600 nm, and 700 nm, the radii of the Airy disk are 2.16 μm, 2.88 μm, and 3.60 μm. The root-mean-square (RMS) radii of the dispersion spot at the central field of view are 1.553 μm, 1.302 μm, and 1.605 μm, respectively, and the RMS radii of the dispersion spot at the marginal field of view are 1.658 μm, 1.515 μm, and 1.678 μm. The simulation results show that the root mean diameter of each wavelength is equivalent to the diameter of the Airy disk, and the light spot is controlled by the size of the Airy disk, which means that the basic aberration correction is close to the diffraction limit.

The relationship between the focusing position and wavelength of the dispersive objective lens group is linearly fitted. The linear determination coefficient R^2 between each wavelength and the focusing position within the working band range is 0.96. The system's design parameters are in the 450 nm–750 nm band range, with 600 nm as the central wavelength. The performance parameters of the designed dispersive lens are shown in Table 1.

Table 1 Performance parameters of the designed dispersive lens.

Parameter	Value
Wavelength (nm)	450–750
Volume numerical aperture	0.13
Maximum measuring angle (°)	±7
Axial measuring range (mm)	20
Average axial resolution (μm)	0.9
Linearity R^2	0.96
Optical length (mm)	330

4. Results and analysis

4.1 Line scan chromatic confocal sensor

The physical system is shown in Fig. 6. The light source is a high-brightness and high-power light emitting diode (LED) light source. A light guide with multiple optical fibers evenly distributed is connected to the end of the light source to provide highly uniform and seamless linear light illumination. All visible light bands are included. The LSCCS consists of a slit and a self-designed dispersion objective lens. The LED light source is integrated and condensed through the optical fiber into a linear light source with a higher light density. After that, it will enter the slit at a certain angle and emerge through the slit in the *X*-axis direction. A linear light with the length of 12.5 mm and a width of 15 μm is formed, and then the measurement light emitted from the slit will be incident on the dispersion objective lens.

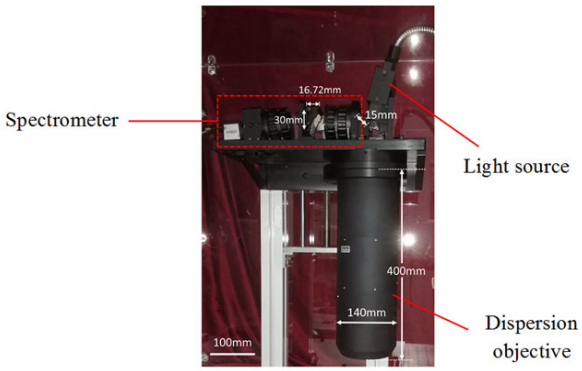

Fig. 6 Line scanning chromatic confocal sensor.

The different colored lights emitted from the dispersive objective lens carry information regarding the surface and thickness of the measured sample, return to the objective lens, and finally enter the spectroscopic system. The spectroscopic system mainly consists of plane reflectors, collimating lenses, prisms, focusing lenses, and complementary metal oxide semiconductor (CMOS) cameras. The reflected light that is emitted from one side of the dispersive objective lens and contains the reflection spectrum information of the surface of the object to be measured is transmitted to the collimating lens through the action of the plane mirror, modulated into a parallel beam and then passes through a prism-grating combination spectroscopic device; here, the grating is a volume phase holographic grating with high diffraction efficiency. Finally, the dispersed reflected light is focused and imaged by the focusing lens and received by the CMOS detector. By analyzing and decoding the spectral data obtained by the CMOS detector, the height

position information of the object's surface to be measured can be obtained.

4.2 System calibration

The spectral wavelength of the LSCCS is calibrated using the AvaSpec-ULS4096CL-EVO spectrometer. The sensor's range, the correlation of the pixel sequence position with the object's depth, and the scanning line length are calibrated using a plane mirror as the object to be measured. The plane mirror's reflectivity for visible light from 450 nm to 750 nm is relatively uniform, and the reflection is over 95%. The specific calibration process is as follows: the reflector is placed on the height displacement stage, starting from the initial calibration position, the displacement stage approaches the dispersion objective lens along the optical axis and continuously moves the reflector within the working range of the system, with a step size of 0.5 mm for each movement; this measurement is repeated 100 times for each calibration point, and the spectral peak wavelength data and displacement value are recorded at this time.

The results from the lowest and highest points that the sensor can measure in the axial range are shown in Figs. 7(a) and 7(b), and the displacement is shown as 20 mm. The range of signals that CMOS cameras can capture is slightly wider than the spectral range of 450 nm to 750 nm. And in practical testing, the longitudinal measurement range of the LSCCS is over 20 mm. To obtain the measurement range of the transverse line scan of the sensor, obstructions are placed on the leftmost and rightmost sides of the reflector, such that a gap is formed in the imaging part, and the measured lateral distance of the system is obtained, as shown in Figs. 7(c) and 7(d). The moving distance of the obstruction is 13 mm; thus, the lateral measurement range of the system is 13 mm. The experimental results of the correspondence between the displacement of the displacement stage and the spectral wavelength are shown in Fig. 8. The linear correlation coefficient between the displacement and the wavelength is R^2=0.96. The maximum allowable tilt angle of the system is determined by using an angular displacement stage at the same height by changing the tilt of the plane mirror. The experimental results show that the maximum allowable tilt angle of the sensor is ±7°.

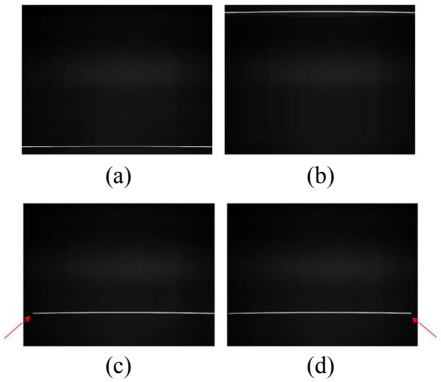

Fig. 7 Images taken by sensors at different positions: (a) lowest and (b) highest points in the axial range that the sensor can measure; the measurement range of (c) leftmost measurement range and (d) rightmost of the sensor along the shape direction.

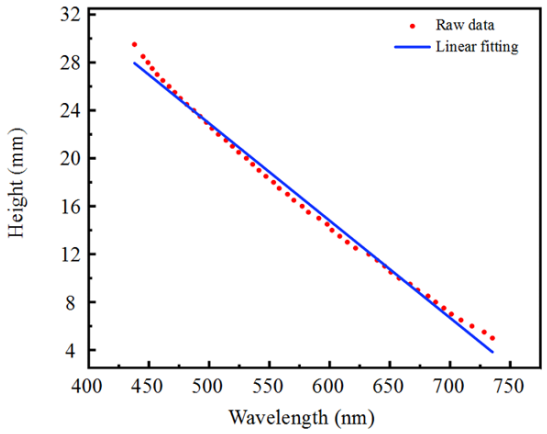

Fig. 8 Depth and wavelength calibration curves.

4.3 Thickness

The standard-thickness glass flat plates are used as the samples to calibrate the thickness detection of the sensor, and the original image is shown in Fig. 9. The axial resolution of the sensor is determined by two factors: the hardware system and the analysis software. Therefore, K9 glass (n=1.516) standard flat samples with 1.0 mm, 1.5 mm, and 2 mm

thicknesses are selected for testing. The thickness error of the samples is 1 μm. Each standard sample is tested ten times, and the peak value of the collected image data is extracted. Combined with the line extraction algorithm, the highest brightness subpixel coordinate of 0.2 pixels can be distinguished. The test results are provided in Table 2. Therefore, the axial resolution of the sensor falls between 0.9 μm and 1.3 μm, exceeding the theoretical value of 0.9 μm. Because the slit is 15 μm wide, which causes an increase in the full width at half maximum (FWHM) of the peak wavelength signal. The slit image broadens and the axial resolution decreases; however, further compressing the slit width can also reduce the incident light flux resulting in a reduction in the signal-to-noise ratio.

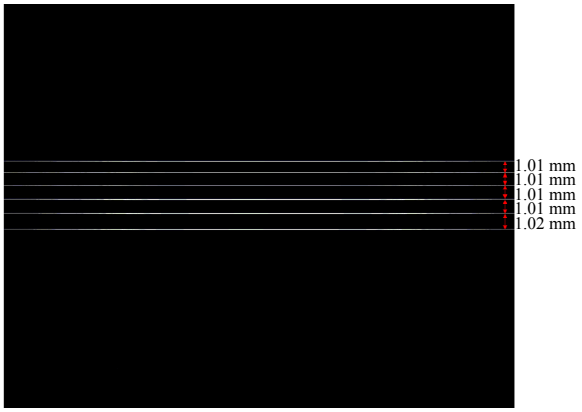

Fig. 9 Image of the multilayer sample.

Table 2 Measured standard deviation and average absolute error.

Wavelength (nm)	Measured standard deviation (μm)	Average absolute error (μm)
460	1.3	1.3
600	1.0	1.0
740	0.9	0.9

The LSCCS is used to detect the thickness of bionic corneal tissue engineering scaffolds. This bionic corneal tissue engineering scaffold is a collagen membrane (Fig. 10) [30]. Collagen membranes are available in wet and dry states; the test results are listed in Table 3. The results show that the LSCCS can be used to monitor the thickness of wet collagen membranes. However, for dry collagen membranes, the monitoring error is significant due to the membrane's unevenness, and a sensor with higher resolution is required.

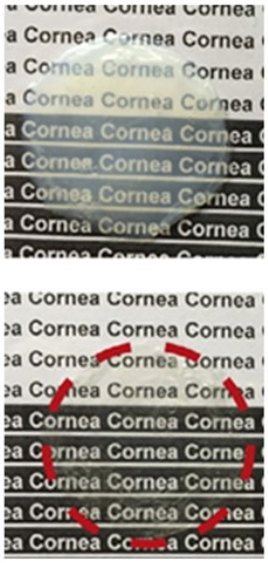

Fig. 10 Wet (up) and dry (down) states collagen membrane [30].

Table 3 Collagen membrane thickness measured standard deviation and average absolute error.

Collagen membrane sample	Measured standard deviation (μm)	Average absolute error (μm)
Wet states	±1.0@5.0 mm thickness	1.0
Dry states	±10.0@0.3 mm thickness	7.0

5. Conclusions

Based on the principle of chromatic confocal and dispersion conditions, under uniaxial conditions, an off-axis dual optical path structure with one side of the same lens tube for incoming light and one side for outgoing light can be used to design a pure spherical dispersion focusing lens group that can achieve significant axial chromatic aberrations. An LSCCS is built using this dispersive objective lens. Based on our experiments, the actual axial measurement range of the measurement system in the 450 nm–750 nm working band is better than 20 mm, and the *X*-direction (linear direction) scanning measurement range is 12.5 mm. The linear coefficient of determination is 0.96. Compared to

the line-scanning spectral confocal measurement systems designed in [9, 16], the approach proposed in this paper not only achieves a 1 μm axial resolution but also provides a larger line field of view and axial measurement range. The system in [9] had the scanning line length of only 8 mm and the measurement range of 2.4 mm, the corresponding resolution in the axial direction, direction of optical fibers layout, and direction of line scanning are 0.6 μm, 10 μm, and 5 μm. Meanwhile, the system described in [16], operating within the wavelength range of 580 nm to 780 nm, achieved a scanning line length of 16 mm, but with a system measurement range of only 0.37 mm. Unlike the traditional point-type chromatic confocal measurement system, our designed LSCCS has higher scanning efficiency and measurement speed. In addition, compared with the existing single-axis chromatic confocal measurement system, our LSCCS avoids the inefficiency of energy loss caused by beam splitting. Finally, the LSCCS is used to measure the thickness of transparent flat glass and the collagen membranes to verify the measurement performance of the system. The relative errors are controlled within 0.7% compared with the contact measurement method results. The proposed system optical path structure design also provides a new concept for achieving the large-range line scanning spectrum confocal measurement technology in the application fields of displacement measurement, surface topography, and transparent material thickness measurement.

Acknowledgment

This work was supported by the Basic and Applied Basic Research Foundation of Guangdong Province (Grant No. 2021A1515011933); Special Project for Research and Development in Key Areas of Guangdong Province (Grant No. 2020B090921002); Science and Technology Innovation Strategy Special Project City and County Science and Technology Innovation Support of Guangdong Province (Grant No. 2023G006).

Declarations

Conflict of Interest The authors declare that they have no competing interests.

Permissions All the included figures, tables, or text passages that have already been published elsewhere have obtained the permission from the copyright owner(s) for both the print and online format.

References

[1] K. Grochalski, M. Mendak, M. Jakubowicz, B. Gapiński, N. Swojak, M. Wieczorowski, *et al.*, "Differences in roughness parameter values from skid and skidless contact stylus profilometers," *Advances in Science and Technology. Research Journal*, 2021, 15(1): 58–70.

[2] W. Gao, H. Haitjema, F. Z. Fang, R. K. Leach, C. F. Cheung, E. Savio, *et al.*, "On-machine and in-process surface metrology for precision manufacturing," *CIRP Annals*, 2019, 68(2): 843–866.

[3] S. L. Dobson, P. C. Sun, and Y. Fainman, "Diffractive lenses for chromatic confocal imaging," *Applied Optics*, 1997, 36(20): 4744–4748.

[4] J. McBride, P. Boltryk, and Z. Zhao, "The relationship between surface incline and con-focal chromatic aberration sensor response," in *O3A: Optics for Arts, Architecture, and Archaeology*, Munich, Germany, 2007, pp. 355–364.

[5] H. J. Tiziani and H. M. Uhde, "Three-dimensional image sensing by chromatic confocal microscopy," *Applied Optics*, 1994, 33(10): 1838–1843.

[6] B. S. Chun, K. Kim, and D. Gweon, "Three-dimensional surface profile measurement using a beam scanning chromatic confocal microscope," *Review of Scientific Instruments*, 2009, 80(7): 073706.

[7] Q. Yu, K. Zhang, C. Cui, R. Zhou, F. Cheng, R. Ye, *et al.*, "Method of thickness measurement for transparent specimens with chromatic confocal microscopy," *Applied Optics*, 2018, 57(33): 9722–9728.

[8] H. M. Park, U. Kwon, and K. N. Joo, "Vision chromatic confocal sensor based on a geometrical phase lens," *Applied Optics*, 2021, 60(10): 2898–2901.

[9] H. Hu, S. Mei, L. Fan, and H. Wang, "A line-scanning chromatic confocal sensor for three-dimensional profile measurement on highly reflective materials," *Review of Scientific Instruments*, 2021, 92(5): 053707.

[10] P. C. Lin, P. C. Sun, L. Zhu, and Y. Fainman, "Single-shot depth-section imaging through chromatic slit-scan confocal microscopy," *Applied Optics*, 1998, 37(28): 6764–6770.

[11] K. Korner, A. K. Ruprecht, and T. F. Wiesendanger, "New approaches in depth-scanning optical metrology," in *Optical Metrology in Production Engineering*, Strasbourg, France, 2004, pp. 320–333.

[12] A. K. Ruprecht, K. Koerner, T. F. Wiesendanger, H. J. Tiziani, and W. Osten, "Chromatic confocal detection for high-speed microtopography measurements," in *Three-Dimensional Image Capture and Applications VI*, San Jose, USA, 2004, pp. 53–60.

[13] S. Chanbai, G. Wiora, M. Weber, and H. Roth, "A novel confocal line scanning sensor," in *Scanning Microscopy*, Monterey, USA, 2009, pp. 351–358.

[14] L. C. Chen, T. Y. Lin, Y. W. Chang, and S. T. Lin, "Chromatic confocal surface profilometry employing signal recovering methodology for simultaneously resolving lateral and axial cross talk problems," in *8th International Symposium on Precision Engineering Measurement and Instrumentation*, Chengdu, China, 2023, pp. 1133−1138.

[15] M. Hillenbrand, A. Grewe, M. Bichra, R. Kleindienst, L. Lorenz, R. Kirner, *et al.*, "Parallelized chromatic confocal sensor systems," in *Optical Measurement Systems for Industrial Inspection VIII*, Munich, Germany, 2013, pp. 222–231.

[16] T. Huang, J. Yang, and T. Ma, "Design of a line-scanning dispersive objective lens for chromatic confocal displacement sensor," in *10th International Symposium on Advanced Optical Manufacturing and Testing Technologies: Advanced Optical Manufacturing and Metrology Technologies*, Chengdu, China, 2021, pp. 186–194.

[17] M. Taphanel and J. Beyerer, "Fast 3D in-line sensor for specular and diffuse surfaces combining the chromatic confocal and triangulation principle," in *2012 IEEE International Instrumentation and Measurement Technology Conference Proceedings*, Graz, Austria, 2012, pp. 1072–1077.

[18] M. Taphanel, R. Zink, T. Längle, and J. Beyerer, "Multiplex acquisition approach for high speed 3D measurements with a chromatic confocal microscope," in *Optical Measurement Systems for Industrial Inspection IX*, Munich, Germany, 2015, pp. 220–227.

[19] J. Seppä, K. Niemelä, and A. Lassila, "Metrological characterization methods for confocal chromatic line sensors and optical topography sensors," *Measurement Science and Technology*, 2018, 29(5): 054008.

[20] K. Niemelä, "Chromatic line confocal technology in high-speed 3D surface-imaging applications," in *Photonic Instrumentation Engineering VI*, San Francisco, USA, 2019, pp. 132–139.

[21] N. Kulkarni, A. Masciola, A. Nishant, K. J. Kim, H. Choi, A. Gmitro, "Low-cost, chromatic confocal endomicroscope for cellular imaging in vivo," *Biomedical Optics Express*, 2021, 12(9): 5629–5643.

[22] R. Ramamurthy and G. Caza, "Performance evaluation of line confocal imaging for surface roughness measurement application," in *Dimensional Optical Metrology and Inspection for Practical Applications X*, Online only, 2021, pp. 50–62.

[23] T. Kim, S. H. Kim, D. Do, H. Yoo, and D. Gweon, "Chromatic confocal microscopy with a novel wavelength detection method using transmittance," *Optics Express*, 2013, 21(5): 6286–6294.

[24] U. Minoni, G. Manili, S. Bettoni, E. Varrenti, D. Modotto, and C. De Angelis, "Chromatic confocal setup for displacement measurement using a supercontinuum light source," *Optics & Laser Technology*, 2013, 49: 91–94.

[25] C. C. Cui, H. Li, Q. Yu, and R. F. Ye, "Design of adjustable dispersive objective lens for chromatic confocal system," *Optics and Precision Engineering*, 2017, 25(4): 343–351.

[26] J. Yang, T. Ma, and T. T. Huang, "Design of chromatic confocal quantitative inverse dispersive objective lens," in *7th Symposium on Novel Photoelectronic Detection Technology and Applications*, Kunming, China, 2021, pp. 2332–2336.

[27] Z. L. Zhang and R. S. Lu, "Initial structure of dispersion objective for chromatic confocal sensor based on doublet lens," *Optics and Lasers in Engineering*, 2021, 139: 106424.

[28] T. Liu, J. Wang, Q. Liu, J. Hu, Z. Wang, C. Wan, *et al.*, "Chromatic confocal measurement method using a phase Fresnel zone plate," *Optics Express*, 2022, 30(2): 2390–2401.

[29] Q. Liu, W. C. Yang, D. C. Yuan, and Y. Wang, "Design of linear dispersive objective for chromatic confocal microscope", *Optics and Precision Engineering*, 2013, 21(10): 2473–2479.

[30] Z. Cui, Q. Zeng, S. Liu, Y. Zhang, D. Zhu, Y. Guo, *et al.*, "Cell-laden and orthogonal-multilayer tissue-engineered corneal stroma induced by a mechanical collagen microenvironment and transplantation in a rabbit model," *Acta Biomaterialia*, 2018, 75: 183–199.